

A new method to correct deformations in emulsion using a precise photomask

M. Kimura^{a,1,*}, H. Ishida^a, H. Shibuya^a, S. Ogawa^a, T. Matsuo^a,
C. Fukushima^a, G. Takahashi^a, K. Kuge^b, Y. Sato^c, I. Tezuka^c, S. Mikado^d

^a*Department of Physics, Toho University, Miyama, Funabashi, 274-8510, Japan*

^b*Chiba University, Chiba, 263-8522, Japan*

^c*Utsunomiya University, Utsunomiya, 321-8505, Japan*

^d*Nihon University, Narashino, 275-8576, Japan*

Abstract

A new method to correct the emulsion deformation, mainly produced in the development process, is developed to recover the high accuracy of nuclear emulsion as a tracking device. The method is based on a precise photomask and a careful treatment of the emulsion films. A position measurement accuracy of 0.6 μm is obtained over an area of 5 cm \times 7 cm. The method allows to measure positions of track segments with submicron accuracy in an ECC brick with as few as 10 reference tracks for alignment. Such a performance can be important for hybrid emulsion experiments at underground laboratories where only a small number of reference tracks for alignment are available.

Keywords:

Nuclear emulsion, Deformation, Photomask

1. Introduction

2 Nuclear emulsions have been used as a particle detector for their excellent
3 submicron spatial resolution, e.g. in experiments studying short-lived parti-
4 cles such as charm and bottom hadrons [1–4] or double- Λ hypernuclei [5, 6].

*Corresponding author

Email address: mitsuhiro.kimura@lhep.unibe.ch (M. Kimura)

¹Now at Albert Einstein Center for Fundamental Physics, Laboratory for High Energy Physics (LHEP), University of Bern, CH-3012 Bern, Switzerland

5 Some recent neutrino experiments also make use of the nuclear emulsions in
6 a hybrid apparatus [7–9]. In such experiments, both production and decay
7 vertices of short-lived particles are reconstructed from the measurements of
8 the parent and daughter particle tracks in nuclear emulsion films. However
9 the practical application of its excellent spatial resolution is limited to an area
10 of a few mm^2 in the vicinity of the interaction and decay vertices because of
11 deformation of emulsion films due to various reasons such as the thermal ex-
12 pansion and distortion of the emulsion layers. This deformation deteriorates
13 the track position measurement accuracy over a larger area. For example, the
14 momentum of a charged particle can be estimated by measuring precisely its
15 multiple Coulomb scattering(MCS) in an Emulsion Cloud Chamber(ECC)
16 brick consisting of emulsion films interleaved with thin metal plates. For a
17 track with a large angle with respect to the perpendicular to the emulsion
18 films, the measurement of its MCS requires precise track position measure-
19 ment over a large area, which is affected by the deformation of emulsion
20 films ². Usually, the effect of the emulsion deformation is corrected by using
21 high momentum reference tracks with a similar angle passing near the track
22 of interest. However, this method cannot be applied in the case, such as in
23 long baseline neutrino oscillation experiments in an underground laboratory,
24 where few references are available. Even though cosmic ray for alignment of
25 ECC brick are irradiated, the angle of their tracks are not necessarily the
26 same as interesting track.

27 In this paper, we present a new method to correct the deterioration in
28 the track measurement accuracy due to the deformation and report on the
29 results of a muon beam exposure which was performed to demonstrate the
30 performance of the method by estimating the momenta of beam muons from
31 their MCS measurements. The method will allow the nuclear emulsion to be
32 used as a tracking device in a wide range of applications such as the emulsion
33 spectrometer technique [13, 14], an emulsion detector placed in a magnetic
34 field, proposed for future neutrino oscillation experiments.

²There are two methods for the MCS measurement in an ECC brick; the “angular”
method [10, 11] and the “coordinate” method [12]. In this paper, the latter is considered
because the application of the former method is limited to low momentum particles.

35 **2. Concept to remove deformations in emulsion**

36 The major part of the deformations in emulsion originates from the devel-
37 opment process. Since the reference marks printed before the development
38 retain their initial positions, we can know the deformations in the emulsion
39 film by comparing measured positions of the reference marks with their de-
40 signed values, then we can subtract them. By this technique, the whole area
41 of an emulsion film will become a position detector with one micron accuracy.

42 We must manufacture a photomask as a printing mask to transfer the
43 reference marks with submicron accuracy to the whole emulsion film. Ref-
44 erence marks in past emulsion experiments were transcribed from a negative
45 film [15] or X-ray sources with 0.1 mm slits [9]. These marks had position
46 accuracy of 10-30 μm and they were used as guides to lead the microscope
47 view to the interested position such as an interaction vertex. The role of
48 our reference marks is completely different from that of the marks in past
49 experiments.

50 The arrangement of the reference marks on the photomask is designed
51 according to the nature of the deformations in emulsion. The deformation
52 size depends on the interested position in an emulsion films: it is small at
53 the central part, but it is large at the edge part. The typical deformation
54 sizes are 0.3 μm within the area of several hundred μm^2 at the center, 1 μm
55 in a few cm^2 and 10 μm in one hundred cm^2 respectively.

56 In order to validate this correction method, we have tried to determine
57 the momentum of beam muons using the MCS measurement, which requires
58 the precise position measurement over a large area in emulsion films.

59 **3. Setup and beam exposure**

60 We carried out a muon beam exposure of an ECC brick at CERN SPS
61 T2-H4 beam line in July 2007. The ECC brick was composed of 28 nuclear
62 emulsion films interleaved with 1 mm thick lead plates as illustrated in Fig. 1.
63 The ECC brick was contained in an acrylic resin box and enclosed in an
64 opaque vacuum bag. Furthermore the brick was enclosed in an extruded
65 polystyrene (STYROFORM[®]) container for heat insulation. The emulsion
66 film is the one developed for the OPERA experiment [16]. It was made of
67 a 205 μm thick triacetyl cellulose (TAC) base with 44 μm thick emulsion
68 layers on both faces. The ECC brick size was 12.5 cm wide, 10.0 cm high
69 and 3.6 cm thick which corresponds to 5 radiation lengths. The ECC brick

70 was exposed to 30, 40 and 150 GeV/ c muon beams and inclined horizontally
71 to the beams with ± 0.3 , ± 0.1 and ± 0.2 rad respectively. A 150 GeV/ c
72 muon beam was exposed perpendicularly for reference. The exposed beam
73 density was controlled to be about $7 \times 10^2/\text{cm}^2$. The beam density is almost
74 uniform in the central region whose size is $3 \text{ cm} \times 3 \text{ cm}$, and it is lower in
75 the surrounding regions. Full width at half maximum of beam profiles are
76 around $7 \text{ cm} \times 7 \text{ cm}$. The beam angular spread was about 1 mrad and its
77 momentum accuracy 1%.

78 The emulsion handling was performed with great care. The ECC brick
79 was dismantled in the dark room soon after the exposure. Grid marks were
80 printed on each emulsion film using a photomask³ made of synthetic quartz
81 with a small thermal expansion coefficient of $5.8 \times 10^{-7} \text{ K}^{-1}$. Grid marks were
82 printed over a $127 \text{ mm} \times 127 \text{ mm}$ area. Figure. 2 shows the design pattern of
83 grid marks on the photomask. Square shape grids, of $5 \mu\text{m}$ ($15 \mu\text{m}$, $400 \mu\text{m}$)
84 side, were printed at intervals of 1 mm (10 mm , 100 mm). The accuracy
85 of the intervals is $0.1 \mu\text{m}$. The printed grid image is shown in Fig. 3. The
86 printed image is not square but rather circular because the light from an
87 electric flash in contact printer is not parallel, it scatters in the emulsion
88 layer, and the contact between the photomask and the film is not perfect.
89 It took only 4.5 hours from the beginning of the exposure to the end of
90 the grid mark printing. Such a fast operation minimizes the emulsion film
91 deformation due to the environmental change during transportation to the
92 processing room. Fig. 4 shows the temperature and the relative humidity
93 variations as a function of time. The maximum changes in the temperature
94 and humidity were 1.5°C and 4.5% respectively.

95 For a typical film, Fig. 5 shows the difference of the grid mark coordinates
96 between the original ones and the measured ones. Each vector shows the
97 size and direction of the displacement, mainly caused by the development
98 processes. Position displacements of a few μm in the central region and
99 larger than $10 \mu\text{m}$ near the edges are observed. This is an example of the
100 deformation that the method described in this paper is aiming to correct.

³The photomask is a chrome coated glass lithographic template designed to optically transfer a pattern to an emulsion layer. The whole size of the glass substrate is $153 \text{ mm} \times 153 \text{ mm} \times 6.35 \text{ mm}$. A chromium oxide layer is deposited over the glass substrate, forming a light shielding film $0.4 \mu\text{m}$ thick. Light transmittance of this layer is about 1%. The pattern on the chromium layer was made by using a photomechanical and etching process.

101 4. Emulsion measurements and analysis method

102 Positions of track segments and grid marks are measured using a fully
103 automated system called Ultra Track Selector (UTS) [17–20]. The UTS is a
104 microscope with a motor controlled three axes stage and an image processing
105 unit. An image is taken by a CCD camera, whose pixel size corresponds
106 to $0.29\ \mu\text{m} \times 0.23\ \mu\text{m}$ on the emulsion film. The positions of the stage are
107 encoded by the LS406 of HEIDENHAIN Co.Ltd. The UTS reads out 16
108 tomographic images through the $44\ \mu\text{m}$ thick emulsion layer, then the image
109 processing unit extracts tracks with a slope smaller than 0.4 rad in the field
110 of view. Just before the track segments are recorded by UTS, grid mark
111 images are taken and automatically recognized. Their center positions are
112 measured by a shape fitting algorithm. The accuracy of grid mark center of
113 $5\ \mu\text{m}$ square size is $\sigma = 0.3\ \mu\text{m}$ in each directions. Only $5\ \mu\text{m}$ grid marks
114 are used to correct the emulsion deformation because their positions can be
115 measured most precisely.

116 An emulsion film is continuously expanding or shrinking under the in-
117 fluence of environmental temperature and humidity, even on the microscope
118 stage. To get rid of this effect, we measured a well-defined reference position
119 of the emulsion film at short intervals during the scanning of an area. We
120 performed measurement of track segments in every $7\ \text{mm} \times 7\ \text{mm}$ area at
121 $2\ \text{cm}$ intervals on the emulsion film. The measurement of the grid marks
122 and the track segments in the central $1\ \text{mm} \times 1\ \text{mm}$ area of each scanning
123 area took about 30 minutes (10 minutes) in the central part (in the edge
124 part) of the film. Position shift in the edge part by the environmental vari-
125 ation is greater than the central ones. That is why the correction must be
126 done more frequently in the edge part. To evaluate the reproducibility of
127 the measurements, all emulsion films were scanned twice in succession. The
128 reproducibility of the track positions is found to be $0.5\ \mu\text{m}$ at one standard
129 deviation.

130 After the scanning, the two corresponding track segments in the emulsion
131 layer on both sides were connected across the $205\ \mu\text{m}$ thick plastic base; so-
132 called base tracks were produced. The position coordinates of each base track
133 are defined as the position of the silver grain closest to the plastic base in
134 the upstream emulsion layer. Base tracks are connected between consecutive
135 emulsion films, then muon tracks are reconstructed over the whole ECC
136 brick. A connection between 2 films was accepted if the positions of the
137 track segments agreed within a tolerance of about $10\ \mu\text{m}$ ($3\ \sigma$).

138 After the connection, the positions of the base tracks of the 150 GeV/ c
139 reference muons are determined with respect to the neighboring grid marks.
140 The printed position shifts $(\Delta x, \Delta y)$ and rotation angle ϕ of the photomask
141 are then calculated, for each film, as the values which minimize the sum of
142 the square of 2D position difference of all the pairs of base tracks between
143 two consecutive films. The minimization process is done by the whole area
144 of the film so as to get larger lever arm for determination of rotation angle.
145 The average difference of the printed positions of the photomask are $\phi_{\text{RMS}} =$
146 3.6 mrad and $(\Delta x, \Delta y)_{\text{RMS}} = (0.30 \text{ mm}, 0.15 \text{ mm})$.

147 Then the original, exposed, track position is recovered by using the near-
148 est grid mark. Since the edge part are severe deformation, we use the nearest
149 grid mark. The deformation correction by using the grid marks are made for
150 2D vector shift. We compare the residuals of muon positions in x direction
151 with or without this correction in Fig. 6. Small, less than $1 \mu\text{m}$, and almost
152 constant residuals are obtained in the central region. We still notice some
153 deterioration of position resolution in the edge region. We think those are
154 mostly due to deformation of the emulsion films in the brick package. Those
155 should be avoided in the future by an improved packing procedure. Mean-
156 while, we confine the rest of the analysis to the central $5 \text{ cm} \times 7 \text{ cm}$ area of
157 the emulsion films. Fig. 7 shows the dependence of the alignment accuracy
158 on the number of reference muon tracks used in the minimization procedure
159 described above. We obtain $0.6 \mu\text{m}$ residual by using 50 or more muon tracks
160 but we note that submicron alignment is achievable with as few as 10 muon
161 tracks.

162 5. Momentum measurements

163 In order to confirm the effectiveness of the above correction method, we
164 evaluated its effect on the determination of the muon momenta of the differ-
165 ent beams from their multiple Coulomb scattering in the brick. The momen-
166 tum of each muon track is estimated from position displacement by multiple
167 Coulomb scattering [12]. The position displacement of each track in one
168 projection is expressed as

$$\delta_i = x_{i+2} - x_{i+1} - \frac{x_{i+1} - x_i}{z_{i+1} - z_i} \cdot (z_{i+2} - z_{i+1}) \quad (1)$$

169 so-called “second difference”, where the base track position at i th film ($i \in$
170 $\{1, \dots, 28\}$) is (x_i, z_i) . Observable root mean square (RMS) of the second

171 difference Δ_{obs} becomes the convolution of the signal of multiple Coulomb
 172 scattering Δ_{sig} and the measurement error ϵ , and Δ_{sig} has the relationship:

$$\Delta_{\text{sig}} = \frac{t}{2\sqrt{3}} \cdot \frac{0.0136(\text{GeV})}{p\beta} \sqrt{\frac{t}{X_0}} \left\{ 1 + 0.038 \ln \left(\frac{t}{X_0} \right) \right\} \quad (2)$$

173 where p and β are the momentum and velocity of the particle, t is the thick-
 174 ness of the material [21]. We use “cell length” as unit of thickness of the
 175 material, cell length = 1 is a 1 mm thick lead plate plus an emulsion film,
 176 used to measure the second difference δ . Fig. 8 shows how to obtain the
 177 second difference as a function of cell lengths. The second differences of cell
 178 length = 1 and 2 are measured by the pattern 1 and 2 respectively.

179 The measurement error ϵ of the second difference is composed of the posi-
 180 tion measurement accuracy of UTS, the alignment accuracy and the position
 181 displacement by the emulsion deformation. There is an approximate relation
 182 of $\epsilon = \sqrt{6} \cdot \sigma_0$ between the measurement error ϵ and the overall track position
 183 measurement accuracy σ_0 at each film after alignment. The distribution of
 184 Δ_{obs} is approximately described by a Gaussian distribution for each muon
 185 track. The momentum of the track is extracted from the observed standard
 186 deviation of this distribution. This determination can in principle be per-
 187 formed for different choices of the cell length. In our analysis, the cell length
 188 was defined as the shortest possible one for which the expected Δ_{sig} exceeds
 189 the estimated measurement error. The application of the correction method
 190 described in section 4 allows to reduce the measurement error and, thus, in
 191 some cases, to reduce the cell length, which further contributes to improve
 192 the momentum resolution.

193 Second differences, the position differences at the film intervals, without
 194 (with) correction in x direction are shown in Fig. 9 for each muon beam,
 195 where the results obtained from a GEANT4 [22] based simulation are over-
 196 laid. The GEANT4 simulation includes residuals obtained from this analysis.
 197 Since an angle of track is larger in y projection, the momentum is estimated
 198 from the second difference in x projection [11]. Total behaviors of second dif-
 199 ferences with respect to the cell lengths are in agreement with the GEANT4
 200 simulation. Fig. 10 shows the second difference distributions scaled to give
 201 $1/p$ for 30 and 40 GeV/ c muons. These distributions are fitted by Gaussian
 202 functions with standard deviations of 77% (64%) and 100% (63%) for those
 203 without (with) correction of 30 and 40 GeV/ c muons, respectively.

204 **6. Conclusions**

205 New correction method of the emulsion deformation has been developed
206 to recover the spatial resolution of the nuclear emulsion over a large area.
207 The method recovers the position resolution deterioration due to the defor-
208 mation mostly in the development process. The method employs a precise
209 photomask, careful treatment of nuclear emulsion, and alignment technique
210 among emulsion films in order to enhance the positioning accuracy. Position
211 measurement accuracy of 0.6 μm is obtained over the area of 5 cm \times 7 cm.
212 The method allows to measure positions of track segments with submicron
213 accuracy in an ECC brick with 10 reference tracks for alignment. It will
214 be applied to long baseline neutrino oscillation experiments where only a
215 few reference tracks for alignment are expected. It will also be useful for
216 other applications of emulsion films as a tracking device such as the emulsion
217 spectrometer technique proposed for future neutrino oscillation experiments.

218 **Acknowledgments**

219 We would like to thank the colleagues of the Fundamental Particle Physics
220 Laboratory, Nagoya University for their cooperation. We gratefully acknowl-
221 edge the financial supports from the Promotion and Mutual Aid Corporation
222 for Private Schools of Japan and the Futaba Electronics Memorial Founda-
223 tion. We thank HOYA corporation for providing the photomask used in this
224 study. For the beam exposure, we acknowledge the support of the SPS staff
225 at CERN. We would like to thank P. Vilain for his careful reading of the
226 manuscript.

227 **References**

- 228 [1] K. Niu, *et al.*, Prog. Theor. Phys. 46 (1971) 1644.
- 229 [2] N. Ushida, *et al.*, Nucl. Instr. and Meth. A 224 (1984) 50.
- 230 [3] S. Aoki, *et al.*, Nucl. Instr. and Meth. A274 (1989) 64.
- 231 [4] K. Kodama, *et al.*, Nucl. Instr. and Meth. A289 (1990) 146.
- 232 [5] S. Aoki, *et al.*, Prog. Theor. Phys. 85 (1991) 1287.
- 233 [6] H. Takahashi *et al.*, Phys. Rev. Lett. 87 (2001) 212502.

- 234 [7] K. Kodama, *et al.*, Nucl. Instr. and Meth. A493 (2002) 45.
- 235 [8] E. Eskut, *et al.*, Nucl. Instr. and Meth. A401 (1997) 7.
- 236 [9] R. Acquafredda *et al.*, JINST 4 (2009) P04018.
- 237 [10] M. De Serio, *et al.*, Nucl. Instr. and Meth. A512 (2003) 539.
- 238 [11] N. Agafonova, *et al.*, New J. Phys. 14 (2012) 013026.
- 239 [12] K. Kodama, *et al.*, Nucl. Instr. and Meth. A574 (2007) 192.
- 240 [13] C. Fukushima *et al.*, Nucl. Instr. and Meth. A 592(2008)56.
- 241 [14] T. Abe *et al.*, JINST 4 (2009) T05001.
- 242 [15] S. Aoki *et al.*, Nucl. Instr. and Meth. A 447(2000)361.
- 243 [16] T. Nakamura *et al.*, Nucl. Instr. and Meth. A 556 (2006) 80.
- 244 [17] S. Aoki *et al.*, Nucl. Instr. and Meth. B 51 (1990) 466.
- 245 [18] T. Nakano, BUTURI 56 (2001) 411 (in Japanese).
- 246 [19] L. Arrabito *et al.*, Nucl. Instr. and Meth. A 568 (2006) 578.
- 247 [20] K. Morishima and T. Nakano, JINST 5 (2010) P04011.
- 248 [21] K. Nakamura, Particle Data Group, *et al.*, J. Phys. G 37 (2010) 075021.
- 249 [22] S. Agostinelli *et al.*, Nucl. Instr. and Meth. A 506 (2003) 250.

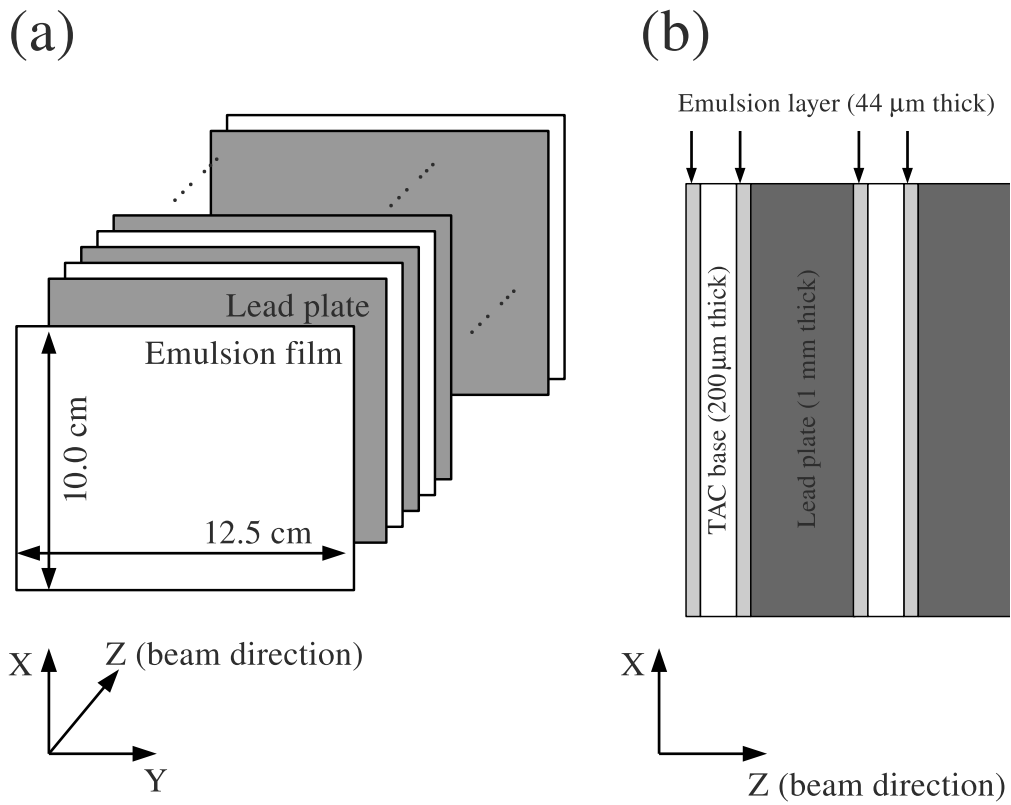


Figure 1: Schematic structure of the ECC brick. (a) Overview and (b) cross view.

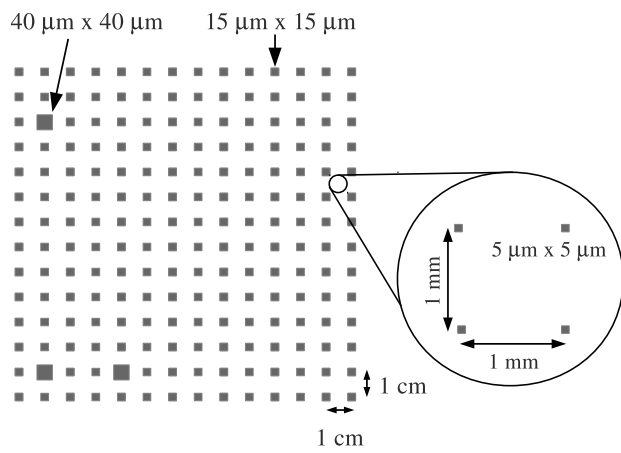


Figure 2: Design pattern of grid mark on photomask. Grid marks of 5 μm square shape are located with spacing of 1 mm. These marks are for the correction of track position. 15 and 400 μm marks are guides to move the microscopic view center to 5 μm marks.

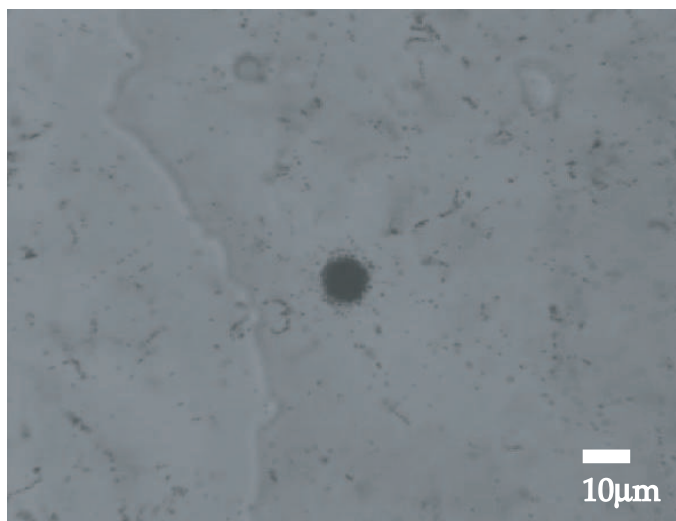


Figure 3: Printed image of a 5 μm grid mark on a film by the contact printing method.

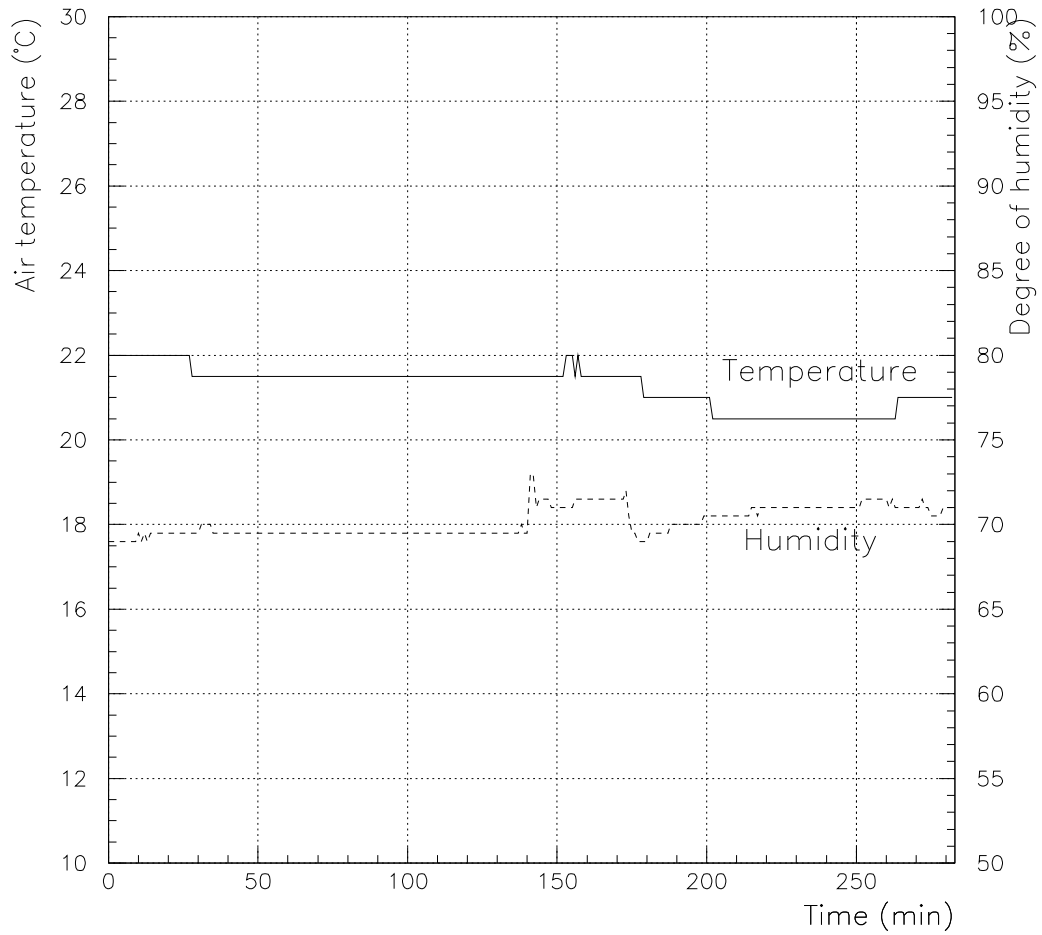


Figure 4: Temperature and relative humidity of the atmosphere surrounding the ECC from the beginning of the beam exposure to the end of the photomask printing. Solid line (dashed line) indicates the temperature (humidity) transition.

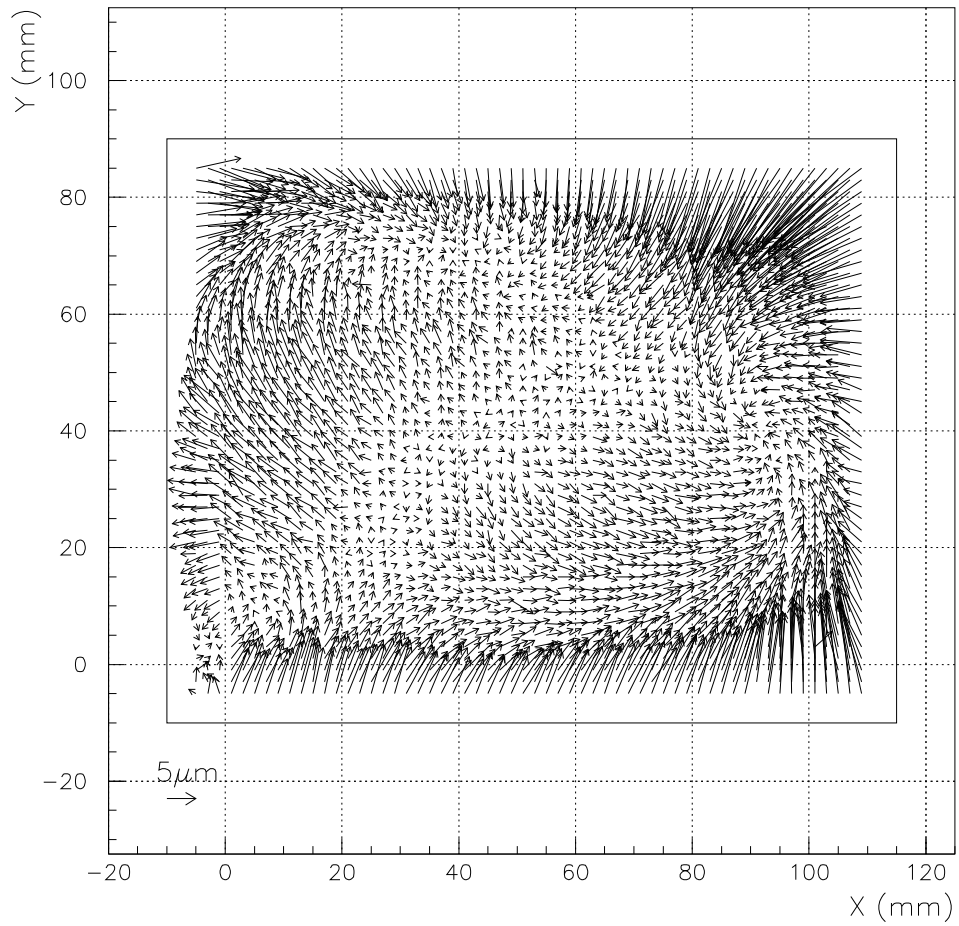


Figure 5: OPERA film deformation reproduced from the grid mark measurements. Each vector shows the position displacement from the original coordinates of the grid mark. Maximum vector size is about 20 μm .

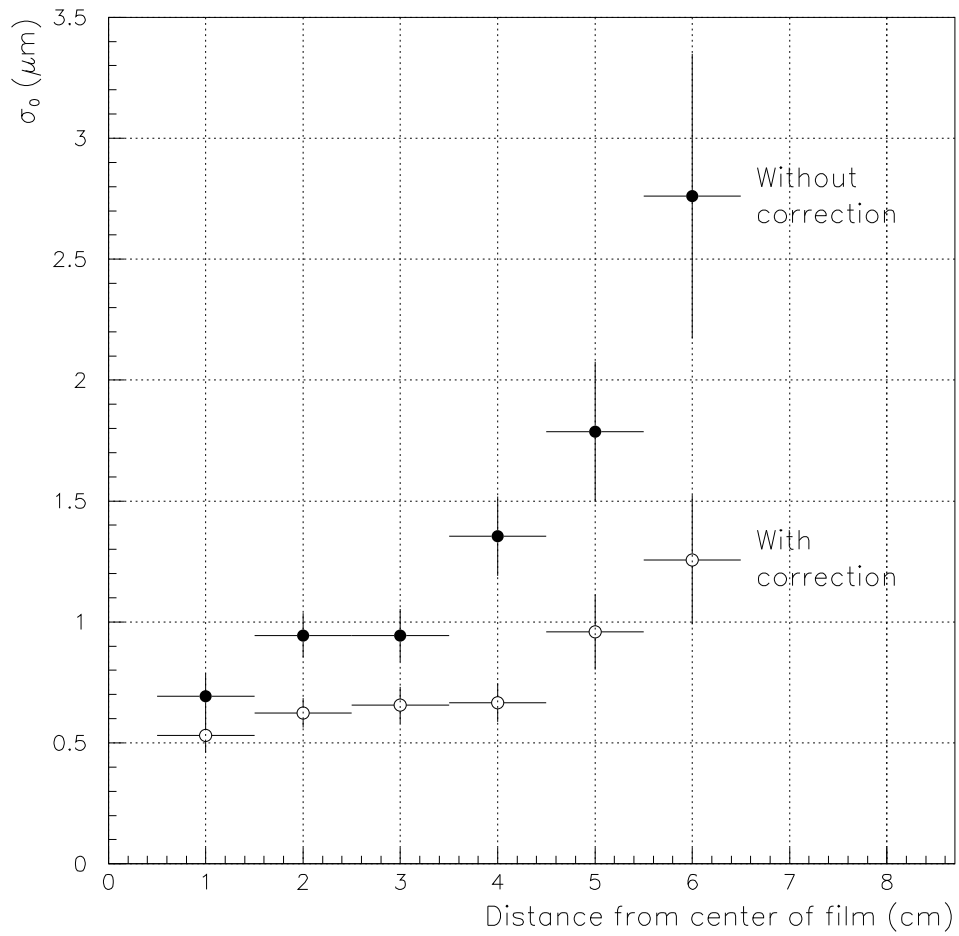


Figure 6: Residuals of track positions σ_0 as a function of distance from the film center. Black (outlined) circles are those without (with) correction.

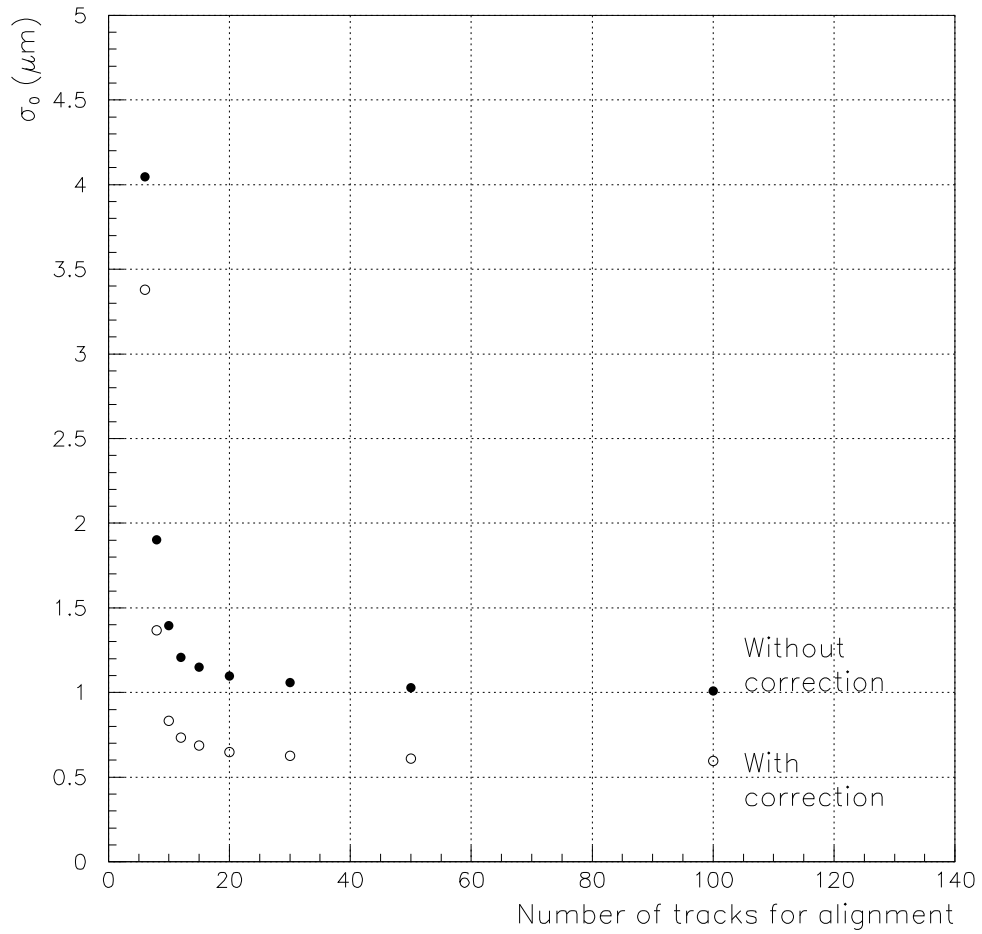


Figure 7: Residuals of track positions σ_0 as a function of number of reference tracks used for alignment. Black (outlined) circles are those without (with) correction.

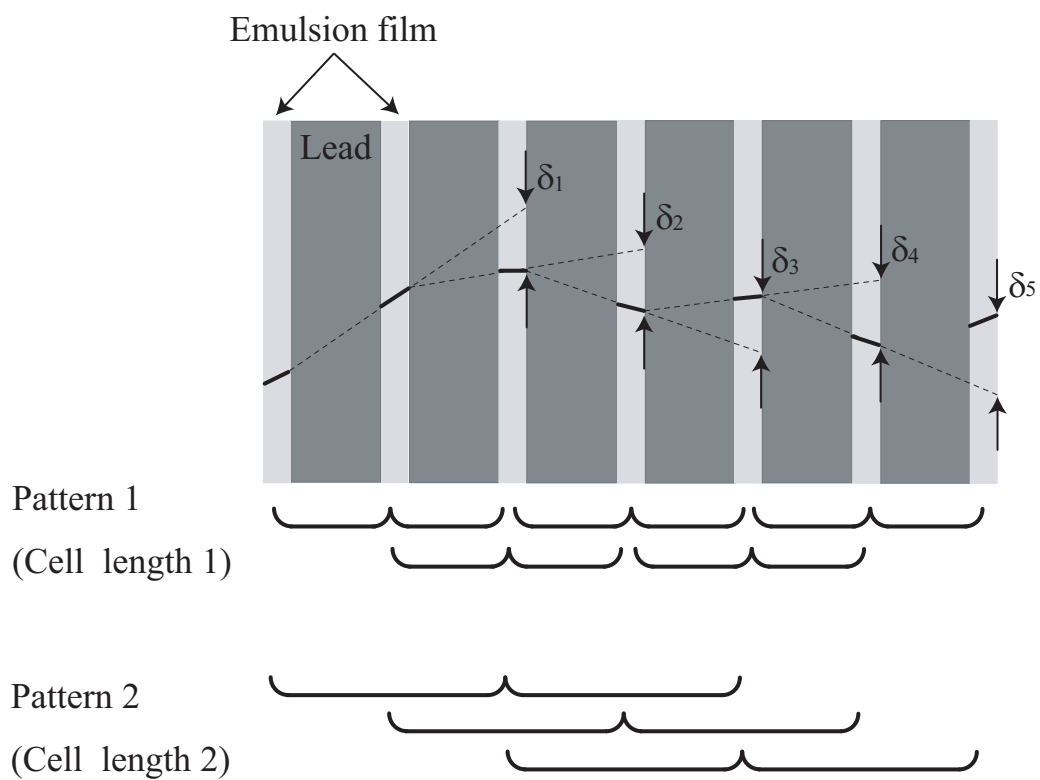


Figure 8: Schematic view of the multiple Coulomb scattering measurement.

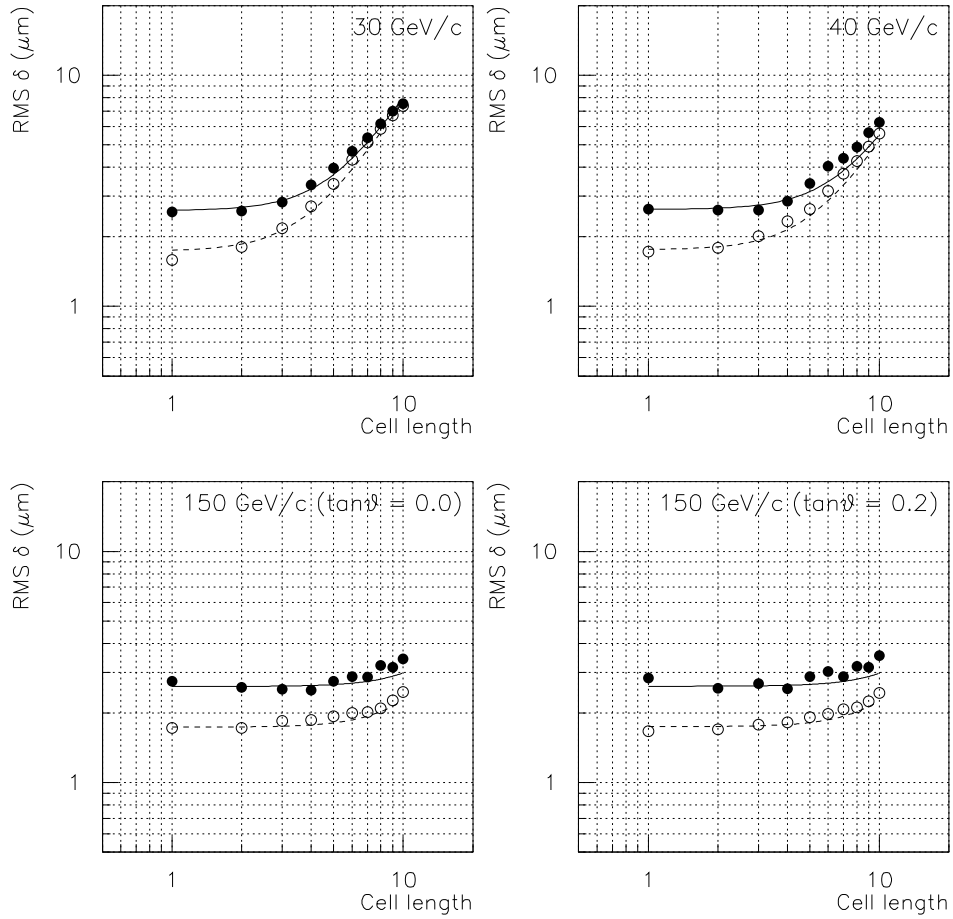


Figure 9: Second difference RMS of muon tracks as a function of thickness of the material in unit of the cell length. Black (outlined) circles show those without (with) correction. Solid (dashed) lines indicate predictions by the GEANT4 simulation without (with) correction.

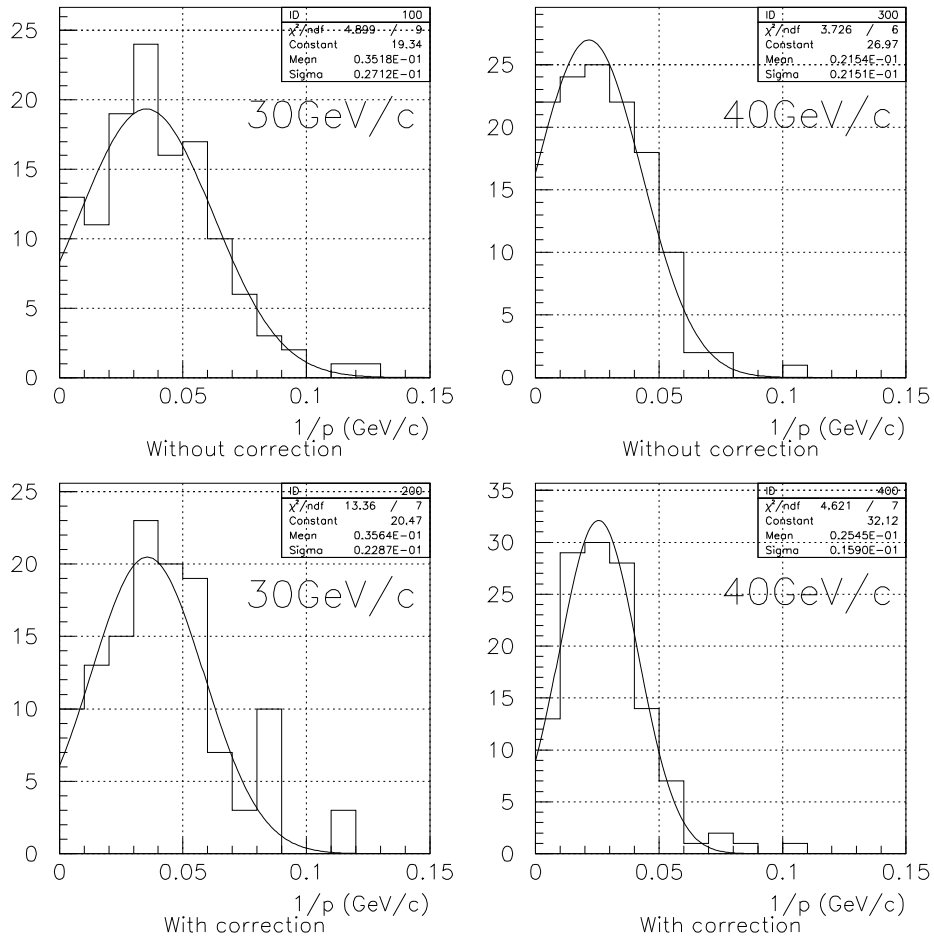


Figure 10: Distributions of the inverse of momenta ($1/p$) for 30 and 40 GeV/c muons. Solid lines represent fit results with Gaussian functions.